Interpretation of the anomalous spectral dependence of the aerosol optical depth of the atmosphere. Part 2. Peculiarities of the aerosol dispersion structure

R.F. Rakhimov, S.M. Sakerin, E.V. Makienko, and D.M. Kabanov

Institute of Atmospheric Optics,
Siberian Branch of the Russian Academy of Sciences, Tomsk

Received April 17, 2000

In this paper we continue our analysis, begun in [S.M. Sakerin, R.F. Rakhimov, E.V. Makienko, and D.M. Kabanov, Atmos. Oceanic Opt. **13**, No. 9, 754–758 (2000)], of the anomalous spectral dependence of the aerosol optical depth of the atmosphere $\tau(\lambda)$, the important peculiarities of which are the following: a decrease of τ in the UV spectral range with a minimum near 0.44 μm and a wide maximum in the range 0.6–0.8 μm; conservatism of the observed spectrum (and, hence, the aerosol microstructure) during 2.5 days. To explain the observed dynamics of $\tau(\lambda)$ we considered the possible scenario of coagulation development of fine aerosol, which is in agreement with delay of the growth of the accumulative fraction. Direct and indirect data are presented on the existence and optical significance of a narrow fraction of medium-disperse particles (~0.3–0.6 μm). A possible mechanism of formation of this fraction is monodispersization of coarse aerosol due to gravitational sedimentation. Results of solution of the inverse problem are discussed for some atmospheric situations (Antarctica, Tomsk, Leningrad Region) which show that the narrow medium-disperse fraction is inherent to the global background aerosol (in the atmospheric column) and plays a dominant role in the formation of the anomalous spectral dependence $\tau(\lambda)$.

Introduction

The situation of an anomalous spectral dependence of the aerosol optical depth (AOD) of the atmosphere, where extremes are observed instead of a power-law decrease with wavelength, was considered in the first part of this paper.[1] A disperse aerosol structure adequate to the anomalous spectrum $\tau(\lambda)$ was revealed by microphysical modeling, and it was shown that the character of the spectral dependence is determined by specific peculiarities of the microstructure of primary and secondary aerosol: a) the diffuse maximum in the "red" spectral range is caused by a narrow medium-disperse fraction with suppressed coarse fraction; b) the power-law decrease of $\tau(\lambda)$ in the UV spectral range is formed by microdisperse particles for low content of the accumulative particles. The main peculiarity of the aerosol structure is its conservatism during ~ 2.5 days with subsequent intense increase in the number density of the accumulative fraction. Our main focus in the second part is on the aerosol physics, i.e., the properties of individual fractions, their processes of transformation, correspondence to physical ideas and experimental facts, and finally issues which were not touched on in the formal solution of the problem.

1. Transformation of the secondary aerosol

Concerning microdisperse aerosol particles, the most important task is to reveal the possible scenario of development that corresponds to the peculiarities of the transformation of $\tau(\lambda)$ from an anomalous dependence to the usual one (low content and conservatism of the accumulative fraction in the first stage and rapid development in the second stage). The aerosol–atmosphere system was modeled by a system of equations representing the dynamics of the integral characteristics of the microdisperse fraction, which is formed from particles in the nanometer size range as result of coagulation growth.

The kinetics of coagulation development of the size spectrum of particles of atmospheric haze is usually described by the Smoluchowski integro-differential equation augmented by terms governing the effects of removal and generation of new particles[2,3]:

$$\frac{\mathrm{d}f_i(x,t)}{\mathrm{d}t} = \frac{1}{2}\int_0^x K(x', x-x')\, f_i(x,t)\, f_i(x-x', t)\, \mathrm{d}x' - f_i(x,t)\int_0^\infty K(x,x')\, f_i(x',t)\ \mathrm{d}x' + \gamma\, f_s(x,t) - \mu\, f_i(x,t), \quad (1)$$

where $K(x, x')$ is the coagulation coefficient of particles with sizes x and x'; $f_i(x', t)$ models the particle size spectrum of the ith fraction; $f_s(x)$ is the spectrum of particles generated by the source; γ is the efficiency of generation of new aerosol; and μ is the efficiency of the particle sink.

Direct solution of the equation for complex spectra $f_i(x, 0)$ is possible only within the framework of numerical iteration methods requiring significant computation time (on the order of a few hours). The

0235-6880/00/09 759-07 $02.00

problem is simplified if one splits the coagulation process into subfractions and integrates the Smoluchowski equation using an effective value of the coagulation constant:

$$K = \frac{4kT}{3\eta}\,[1 + \exp\,(1/2b_i) +$$

$$+ l_0\, C_{\mathrm{Khi}}\,\{\exp\,(1/4b_i) + \exp\,(5/4b_i)\}/r_i], \quad (2)$$

where k is the Boltzmann constant, T is temperature, η is the viscosity of air, l_0 is the mean free path of the molecules, C_{Khi} is the Cunningham correction,[3] r_i and $1/b_i$, respectively, are the characteristic size of the coagulating aerosols and the width of the mode of their size distribution (see Ref. 1, Eq. (5)).

As result, we arrive at a system of differential equations describing the dynamics of the total number density of the ith particle fraction[2]:

$$\frac{\mathrm{d}N_i}{\mathrm{d}t} = \frac{K}{2}\,N_i^2 - \mu\,N_i + \gamma\,N_{\mathrm{s}}\,. \quad (3)$$

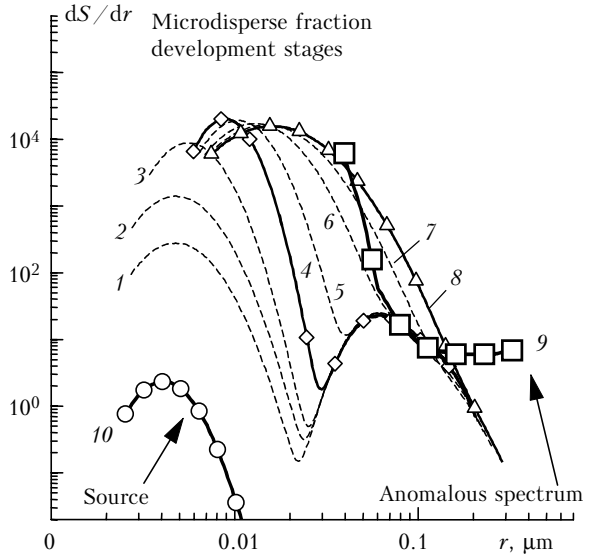

Fig. 1. Temporal dynamics of the coagulation development of the size spectrum of the fine aerosol fraction.

Analogous equations can be obtained for the first (L_i) and second (W_i) moments of the spectra from Eq. (1), if we multiply by x and x^2 and integrate within the above limits:

$$\frac{\mathrm{d}L_i}{\mathrm{d}t} = -\,\mu L_i + \gamma\,L_{\mathrm{s}}\,; \quad (4)$$

$$\frac{\mathrm{d}W_i}{\mathrm{d}t} = -\,\frac{K}{\pi}\,L_i^2 - \mu W_i + \gamma\,W_{\mathrm{s}}\,; \quad (5)$$

where N_{s}, L_{s}, and W_{s} are the corresponding integral characteristics of the size spectrum of particles generated by the source. Next, the temporal dynamics of the integral characteristics [solutions of Eqs. (3)–(5)] were used to predict the structural changes of the size spectrum under the combined effect of processes of generation of particles in the nanometer size range and their subsequent coagulation and removal from the local cell. The development of aerosols of only the new generation is illustrated in Fig. 1 as the sequence of curves *1–8* (curve *10* shows the spectrum of generation of nanometer-size particles). The size spectrum of the accumulative fraction (second mode of curve *4*) is shown in Fig. 1 for comparison.

Our calculations show that one can distinguish three stages in the process of development. Quantitative accumulation of nanometer-size particles (*1–3*) with size spectrum analogous to the spectrum of the source generation $s_{\mathrm{s}}(r)$ occurs in the first stage. When the number density $N^{(1)}(t_1)$ reaches a certain level, the stage of active coagulation begins. The size spectrum is continuously deformed, and the modal radius reaches the value r_{m1} (curve *4*).

The resulting spectrum for intermediate source strength acquires a tendency toward narrowing already in the second stage, but within certain limits. The increase in the number density $N(t)$ is accompanied by a decrease in the rate of increase, and when a certain quasi-stationary level $N^{(2)}$ has been reached, narrowing of the size spectrum ceases and the second stage terminates.

If the source strength and the efficiency of coagulation growth of particles are sufficiently high, the spectrum $\mathrm{d}S/\mathrm{d}r$ in the third stage continues to move up the size scale. The tendency toward narrowing of the spectrum is replaced by a tendency toward broadening (curves *5–8*). At some time t_2 the periphery of the distribution of the microdisperse fraction reaches the size range of the accumulative fraction (curve *6*). Starting at this point, the initially anomalously low content of the submicron fraction increases (curve *9*) and displays an increasingly greater optical significance. As a result of this process, the anomalous dependence $\tau(\lambda)$ transforms to the usual one. The values of the above parameters $N^{(1)}$, $N^{(2)}$, t_1, t_2, r_{m1} depend on the efficiency of coagulation of the particles, as well as on specific peculiarities of the generation source $s_{\mathrm{s}}(r)$.

The presented model estimates of the formation and development of the small-particle fraction are in agreement with the rate of transformation of $\tau(\lambda)$ during the experiment and explain the constancy of the shape of the spectral behavior of AOD during the first two days, which coincides approximately with the value $t_2 \cong 62$–67 hours. When comparing the field data and the modeling results, it should be borne in mind that coagulation development of the nanometer-size particles is effective only under conditions where their number density remains sufficiently high, i.e., near the source. If a cell of aerosol–gas mixture has detached from the zone of effective action of the source (under the influence of turbulent mixing), not only does the rate of particle generation from the gas phase decrease, but the particle number density also decreases quite rapidly. In addition to this, the rate of the coagulation process decreases. Thus, the longer the cell is present in the zone of effective action of the source, the higher the level of coagulation development the disperse system will reach.

Aerosols at different stages of development are mixed during turbulent emission of particles of the microdisperse fraction. A size spectrum is thereby formed that is a superposition of spectra of different ages of coagulation. Thus the optical contribution of the microdisperse fraction, as well as the process of reconstruction of the "normal" effect of the accumulative fraction, is determined not only by the efficiency of coagulation transformation of the aerosol size spectrum, but also by its vertical development, which depends on synoptic conditions.

2. Peculiarities of the spectrum of large particles

As was mentioned above, extended duration of the anomalous spectral dependence of AOD (see Ref. 1, Fig. 1) is possible only under conditions of conservatism of the aerosol size spectrum in the atmospheric column as whole. The stability of the disperse structure of aerosols of the secondary generation ($r < 0.4$ μm) can be explained by the comparatively low rate of coagulation development and the low efficiency of filling of the interval of accumulative fractions by new particles (see above). Taking the meteorological conditions into account (Ref. 1, Table 1), the small contribution and "delayed" development of the coarse fraction appear to be natural. The moistened soil (after rain on July 23 and 24), low values of the temperature and wind velocity, as well as anticyclonic conditions, apparently prevented filling of the atmosphere by aerosol from the underlying surface.[4,5,etc] The unexpected result against this background is the high optical significance, stability, and pronounced narrowness of the particle distribution in the range of medium-disperse particles.

Analysis of the data in the literature shows that the mode of medium-disperse particles was repeatedly observed in some layers of the atmosphere, but did not attract attention because of its small optical significance against the background of other fractions. The data of airborne measurements in "non-condensed clouds"[6] and in the near-ground layer of the atmosphere[7] can be considered as manifestations of this fraction (Figs. 2*a*, *b*).

From the standpoint of formal similarity to $\tau(\lambda)$ we should mention a number of papers which attempt to interpret data on the optical characteristics of smoke aerosols.[8–10] In common with these results (called the effect of spectral blueing and a "blue Sun") is the extinction minimum near 0.4 μm and the maximum in the "red" spectral range. There is also agreement in the microstructural interpretation of the effects – the conclusion is drawn that a narrow fraction of particles with $r_m = 0.31–0.44$ μm is present in the atmosphere. (However, in the explanation of this effect it was not indicated whether the observed optical anomaly is the consequence of a manifestation of the principal maximum of K_ε). Despite the outward similarity to $\tau(\lambda)$, the atmospheric conditions in the situation of a smoke aerosol are significantly different – large optical depth, the presence of aerosol absorption, etc. Note that in our case the important role of the medium-disperse fraction of the clear atmospheric column in the optical properties is established by microphysical modeling and solution of the inverse problem (see below).

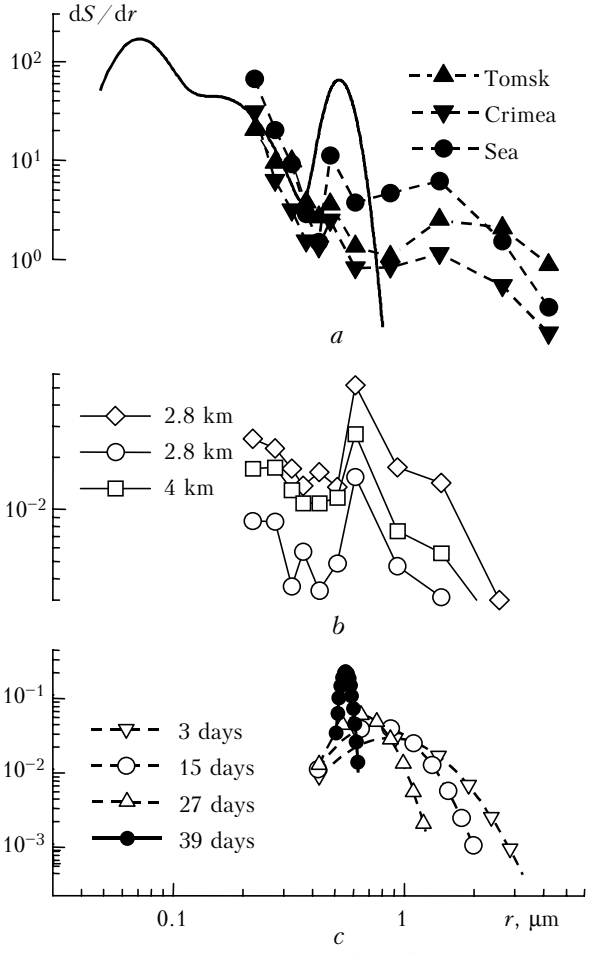

Fig. 2. Manifestations of the medium-disperse fraction in different layers of the atmosphere: a) results of measurements in the near–ground layer,[7] the solid line shows model calculations for the anomalous dependence $\tau(\lambda)$; b) airborne measurements inside a "non-condensed cloud"[6]; c) temporal dynamics of the aerosol microstructure during gravitational sedimentation (stratosphere, at a height of 21 km).

Let us try to explain the nature of the narrowness and high optical significance of the medium-disperse particles, considering the results of the model estimates on transformation of stratospheric aerosol.[11] The hypothesis is proposed for the first time in this paper that the size spectrum of the coarse particles at some altitudes in the stratosphere shows a tendency toward monodispersization (Fig. 2*c*) under weak turbulent mixing and the Stokes sedimentation effect. The change in the disperse structure of the eruptive cloud was modeled by the following system of equations for the integral indicators:

$$\frac{\partial \hat{Q}_i(z,t)}{\partial t} = \frac{\partial}{\partial z} D(z) \frac{\partial \hat{Q}_i(z,t)}{\partial z} - \frac{\partial}{\partial z} [W_{Q_i}(z) \hat{Q}_i(z,t)], \quad (6)$$

where the vector-parameter $\hat{Q}_i(z, t)$ characterizes the correlated changes of three quantities: the volume $V_i(z, t)$, surface $S_i(z, t)$, and number $N_i(z, t)$ densities; $W_{Q_i}(z)$ is the mean rate of Stokes sedimentation of particles of the ith fraction estimated for each equation from the modal radius of the distribution density function of the respective integral indicator.

The model estimates based on system of equations (6) show that a very narrow mode is formed at some heights from the composition of the coarse fraction during gravitational sedimentation of the eruptive cloud. The effect of monodispersization was observed during the aerosol sedimentation process consecutively at different heights, but the particle size spectrum always narrows to the same range with $r_m = 0.50-0.55$ μm (obviously, the most "favorable" under the physical conditions of the atmosphere). Thus, there are reasons to suppose that the more narrow medium-disperse mode is formed from a wide spectrum of coarse particles during gravitational removal (taking into account the viscosity of the carrier medium). The favored preservation of medium-disperse particles in the atmosphere up to the Junge layer in the stratosphere may be the primary cause of the stability of the maximum of $\tau(\lambda)$ in the range 0.6-0.8 μm and the low mobility of this mode during the subsequent measurement days.

The considered formation of the narrow fraction is in agreement with the data of the model calculations,[5] namely, the end result of taking into account the totality of dynamic processes in the troposphere (removal, wash-out of aerosol, etc.) is monodispersization of soil aerosol in the range of medium-disperse particles.

3. Solution of the inverse problem

To solve the inverse problem, we use the representation provided by Eq. (4) in Ref. 1, assuming that the effective height $H_0 \approx 1$ km, i.e., a value close to the mean estimates.[12] It then becomes possible to determine the particle distribution function by solving the system of equations for the aerosol extinction coefficients $\beta_\varepsilon(\lambda)$:

$$\int_{R_1}^{R_2} K_\varepsilon(r, \lambda_i)\, s(r)\, dr = \frac{\tau(\lambda_i)}{H_0} = \beta_\varepsilon(\lambda_i), \quad i = 1, \ldots, n, \qquad (7)$$

where $s(r) = \pi r^2\, dN/dr = \pi r^2 f(r)$; $f(r)$ is the particle size distribution function; and $K_\varepsilon(r, \lambda_i)$ is the extinction efficiency factor. To invert Eq. (7), we applied the regularization algorithm[13] in which the approximate solution vector s^* is determined by direct minimization of the smoothing functional T_α in k-dimensional space. In the regularization by the Tikhonov method the functional T_α is written in the form

$$T_\alpha(s) = \sum_{i=1}^{n} \left(\sum_{l=1}^{k} Q_{\varepsilon,il}\, s_l - \beta_{\varepsilon,i} \right)^2 + \alpha\, \Omega(s), \qquad (8)$$

where s_l are the components of the solution vector; $Q_{\varepsilon,il}$ are the matrix elements calculated by the quadrature formulas[14] for the efficiency factor $K_\varepsilon(r, \lambda_i)$ on the fixed grid r_l ($l = 1, 2, \ldots, k$) and λ_i ($i = 1, 2, \ldots, n$); α is the regularization parameter; $\Omega(s)$ is the smoothing functional, whose form is determined by the character of the restrictions imposed on the desired solution.[15] The parameter α was determined on the basis of an analysis of the behavior of the norm of the deviation of two consecutive regularized solutions $\| s_{\alpha,j} - s_{\alpha,j-1} \|$ on a grid of decreasing values of α. This approach corresponds to the criterion of finding a quasi-optimal value of the regularization parameter.[15] Selection of the parameter α by the discrepancy method[15] turned out to be less suitable in this case because of strong "smoothing" of the solution for the anomalous dependence $\tau(\lambda)$. The estimate of the right boundary of the size spectrum R_2 was found according to recommendations in Ref. 16 from the relation:

$$(R_2)^{-1} \int_{R_1}^{R_2} K_\varepsilon(\lambda_{max}, r)\, dr = \overline{K}_m\, \beta(\lambda_{max})/\beta_{max}, \qquad (9)$$

where $\overline{K}_m = \beta_{max}/S$ is the polydisperse extinction efficiency factor at the maximum of $\beta_\varepsilon(\lambda)$; $S = \int_{R_1}^{R_2} s(r)\, dr$. The estimate of the boundary R_2 obtained from Eq. (9) was then found more exactly by the iterative procedure proposed in Ref. 16.

Before considering the specific results, let us recall factors which increase the error. It was noted earlier that the use of the approach based on "an effective height H_0 common to all fractions" can lead to a "distortion" of the inversion results, namely, the distribution functions dS/dr. In addition, the short UV part of $\tau(\lambda)$ has an increased error ($\delta_\tau \sim 0.01$) and carries too little information for reliable reconstruction of the microstructure in the small-particle range ($r < 0.2$ μm). Therefore let us focus on the parameters of the medium-disperse fraction, which determines the anomalous behavior of $\tau(\lambda)$. Results pertaining to the disperse structure of the secondary aerosol will be considered in Part 3.

Results of solution of the inverse problem for different ways of prescribing the initial data (Fig. 3*a*) are shown in Fig. 3*b*: curves *1* and *2* show $\tau(\lambda)$ during the first day of the anomaly and the mean value of $\tau(\lambda)$ during the "conservative" period, respectively; curves *3* and *4* present two variants of the possible spectral behavior of the medium-disperse component of AOD $\tau_{med}(\lambda)$. In this case, when prescribing $\tau_{med}(\lambda)$, we restrict ourselves to approximate estimates based on the data obtained from direct microphysical modeling (see Ref. 1, Fig. 3*d*), i.e., it was assumed that $\tau(\lambda)$ is determined in the "red" spectral range by the values of the medium-disperse component ($\tau \approx \tau_{med}$). The spectral behavior of $\tau_{med}(\lambda)$ in the short-wavelength range is neutralized and has a small maximum in the range of the second maximum of the extinction efficiency factor K_ε.

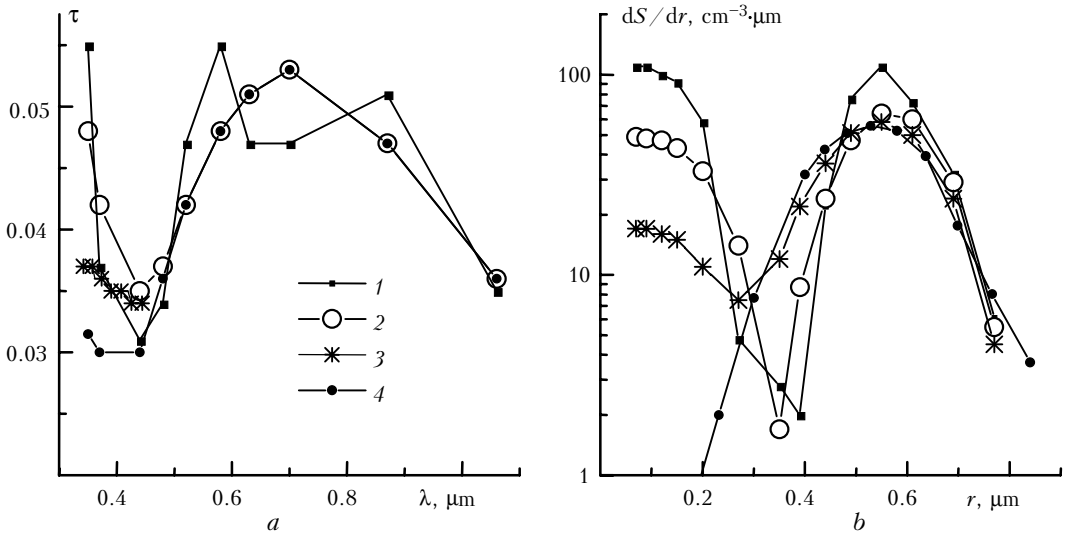

Fig. 3. Illustration of the results of solving the inverse problem for different initial data: τ(λ) on July 24 (*1*); mean smoothed dependence τ(λ) on July 24–26 (*2*); two ways of selecting the medium-disperse component $\tau_{med}(\lambda)$ (*3*) and (*4*).

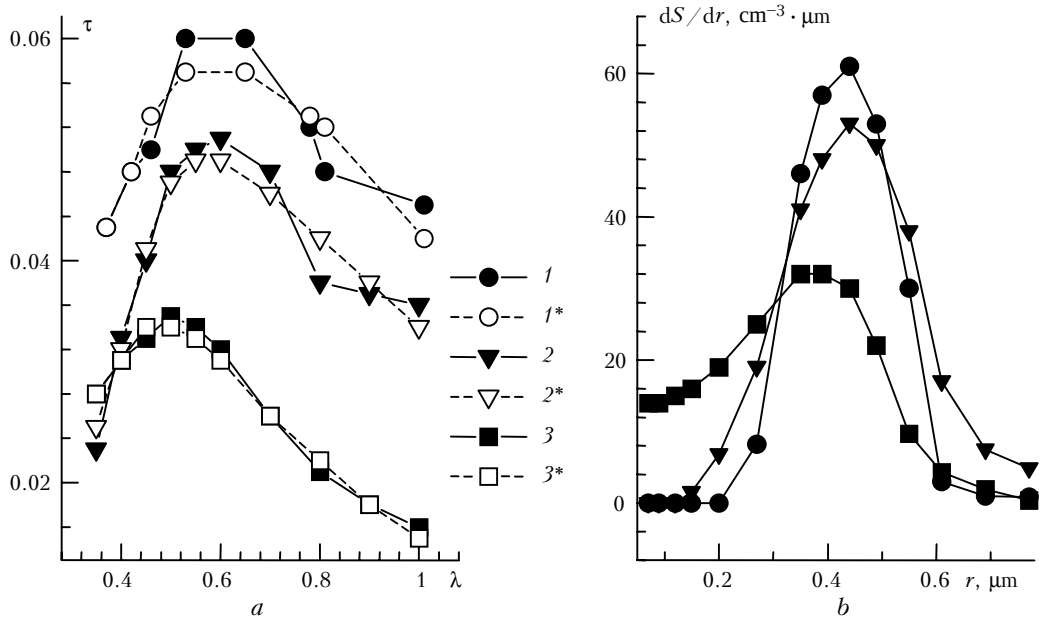

Fig. 4. Results of reconstructing the aerosol microstructure for situations of a background aerosol: Sosnovo, Leningrad region[18] (*1*); Vostok station (winter) (*2*), and Mirnyi station (summer)[17] (*3*); curves *1**, *2** and *3** are the results of the inverse transformation [the values τ(λ) are calculated from the reconstructed distribution functions dS/dr].

Table 1. Parameters of the medium-disperse mode approximated by the log-normal distribution

Region	r_m, μm	b_i	ln σ	N, cm^{-3}	S, μm^2 · cm^{-3}	V, μm^2 · cm^{-3}
Vostok (winter)	0.35	6.7	0.075	6.03	9.04	1.23
Mirnyi (summer)	0.38	4.3	0.116	9.02	15.38	2.45
Sosnovo	0.40	15.2	0.033	6.84	13.56	1.93
Tomsk, July 24–26	0.53	29.5	0.017	3.69	12.77	2.32

The examples in Fig. 3 show that despite the supposed distortions (see above), the desired mode is reconstructed in all cases in approximately the same way, at least in the mid-range and in the range of large particle sizes. Differences appear only in the left wing of the mode and in the finely-dispersed range.

Hence, there is reason to compare the selected fraction with the results of inverting other analogous data, first of all with the Antarctic, where the considered dependence τ(λ) is typical. The results of inverting τ (Fig. 4*a*) in principle gave the expected result: the distribution functions $s(r) = dS/dr$

(Figs. 3*b* and 4*b*) are similar to each other and are located within a relatively narrow size range.

To quantitatively characterize the medium-disperse fraction, the obtained data were approximated by the log-normal distribution. It is important here to find not the best approximation function but to use a generally accepted form for uniform description of dS/dr in different regions. The main parameters of the distribution – the modal radii r_m and the number, surface and volume densities of particles (N, S, V), as well as b_i (see Ref. 1, Eq. (5)) and $\ln\sigma$ characterizing the half-width of the mode, are presented in Table 1. In spite of some differences, the results obtained in Tomsk and Sosnovo[18] during the period of the anomaly are similar to the disperse composition of the aerosol in the clearest region – the Antarctic.

4. Correspondence to the background situation

Rounding out the exposition of Part 2 of this paper, let us consider one more question – to which state of the aerosol atmosphere does the anomalous dependence $\tau(\lambda)$ correspond?

It was concluded earlier[4,17] from the results of observations in the Antarctic as well as some other cases of high atmospheric transparency (see the generalization in Ref. 1, Fig. 2) that the characteristic dependence of $\tau(\lambda)$ with a maximum in the "red" wavelength range is inherent to the background aerosol and has a global character. Judging from the complex of general indicators (atmospheric conditions, spectral behavior, and the value $\tau \approx 0.04–0.08$), the similarity of the "Tomsk" results to the background aerosol criteria is obvious. Besides, the results of the inversion (see Table 1) allow us to back up existing ideas with quantitative estimates. Taking into account differences in the notions of the background aerosol (regional, between volcanic eruptions, etc.[4,5]) it is necessary to explain that our attention in this case is focused on: a) aerosol of the entire atmospheric column; b) optically significant fractions which determine the influx of solar radiation, c) peculiarities of the minimum in the configuration of the aerosol disperse structure which is mainly formed not as a result of local sources but by the combined effect of all sources, along with various processes of aerosol transfer and transformation. The regions of the Antarctic correspond to this notion most completely.

Indeed, with increasing distance from the primary and secondary aerosol sources (including in the vertical direction), a redistribution of the roles of separate fractions occurs in the initially quasi-continuous total size spectrum, the role of the coarse fraction decreases significantly, the content of Aitken particles decreases (a deficit of accumulative particles is the consequence), and the narrow mode of medium-disperse particles becomes optically significant. Actually, the particles in this size range (~0.3–0.6 μm) determine the spectral peculiarities of radiation extinction under background conditions. The key point here is not to determine the nature or composition of the narrow medium-disperse mode ("aged" accumulative fraction or the result of sedimentation of the coarse fraction, as was shown in Section 3), but to marshal facts that are evidence of a stable and favored preservation of the particles in this size range in the atmosphere.

Similar values of the position of the optically significant fractions: 0.53 μm[19] and ~ 0.35 μm (second insignificant mode at ~ 0.65 μm)[18] are presented in the data available in the literature on inverting the "background" dependences.

As for the fine aerosol ($r < 0.2$ μm), its weak manifestation at the boundary of the wavelength range ($\lambda < 0.44$ μm) is revealed only under continental background conditions (in distinction to the clearer Antarctic air).

Taking into account the content of the discussions of this paper, we think it necessary to explain the terminology. The notions "background", "global", and "anomalous" are used here as a convenient combination of indicators characterizing the most significant peculiarities of the object of study as well as the factors governing the formation of the atmospheric situation. Correspondence to a *background* situation characterizes some minimum level of τ and of the aerosol content of the atmospheric column. Introduction of the term *global* is motivated by a desire to emphasize that the considered disperse structure (and corresponding AOD of the atmosphere) is the result of the formation and spread of aerosol on a planetary scale rather than the effect of isolated sources. The term *anomaly* defines a situation in which the spectral dependence $\tau(\lambda)$ and the aerosol particle size distribution function are qualitatively different from their "normal" values typically observed in most regions under most atmospheric conditions. (These clarifications reflect our ideas on the problem, but not our priority in interpreting these terms.)

Conclusion

Summarizing the results of the model calculations of the aerosol disperse composition adequate to the anomalous dependence $\tau(\lambda)$ taking into account the peculiarities of its subsequent transformation to the "normal" spectral dependence, we note the following:

a) The considered scenario of coagulation development of the fine aerosol fraction is in agreement with the real-world dynamics of $\tau(\lambda)$ and includes three stages of the process: 1) accumulation of particles of nanometer size; 2) narrowing of the size spectrum; 3) broadening of the spectrum to the size range of the accumulative mode if the source strength and the efficiency of coagulation are sufficiently high.

b) Optical significance of the narrow medium-disperse fraction of particles (~0.3–0.7 μm) is demonstrated on the basis of a comparison of direct microphysical data (known *a priori*) and results of

modeling and inversion of the spectra $\tau(\lambda)$ for background conditions; also its most probable mechanism of formation is considered (monodispersization resulting from gravitational sedimentation).

c) The parameters of the medium-disperse mode inherent to the background global aerosol (of the atmospheric column) and determining the value of the radiation influx under the clearest conditions (r_m = 0.35–0.53, N = 3.7–9 cm^{-3}) are determined. Comparison with the data obtained in the Antarctic shows that the "Tomsk" results correspond to the background situation both in the value of τ (~ 0.04) and of the medium-disperse component, but reveal a difference in the finely dispersed particle content.

Acknowledgments

This work was supported in part by Russian Foundation for Basic Research (Grants No. 98–05–03177a and 00–03–32422a).

References

1. S.M. Sakerin, R.F. Rakhimov, E.V. Makienko, and D.M. Kabanov, Atmos. Oceanic Opt. **13**, No. 9, 754–758 (2000).
2. R.F. Rakhimov, Atm. Opt. **2**, No. 3, 206–212 (1989).
3. S.K. Friedlander, *Smoke Dust and Haze: Fundamentals of Aerosol Behavior* (Wiley Interscience, New York, 1977), 386 pp.
4. K.Ya. Kondrat'ev, ed. *Aerosol and Climate* (Gidrometeoizdat, Leningrad, 1991), 542 pp.
5. K.Ya. Kondrat'ev and D.V. Pozdnyakov, *Aerosol Models of the Atmosphere* (Nauka, Moscow, 1981), 104 pp.
6. V.E. Zuev, B.D. Belan, and G.O. Zadde, *Optical Weather* (Nauka, Novosibirsk, 1990), 194 pp.
7. V.S. Kozlov, V.V. Polkin, and V.Ya. Fadeev, in: *Abstracts of Reports at Second Conference on Atmospheric Optics*, Tomsk (1980), pp. 182–185.
8. G.S. Golitsyn, A.K. Shukurov, et al., Izv. Akad. Nauk SSSR, Fiz. Atmos. Okeana **24**, No. 3, 227–233 (1988).
9. I.N. Sokolik, Izv. Akad. Nauk SSSR, Fiz. Atmos. Okeana **24**, No. 3, 274–279 (1988).
10. R. Wilson, Monthly Notices Roy. Astron. Soc. **III**, 478 (1951).
11. R.F. Rakhimov, Atmos. Oceanic Opt. **5**, No. 5, 343–348 (1992).
12. V.E. Zuev and G.M. Krekov, *Optical Models of the Atmosphere* (Gidrometeoizdat, Leningrad, 1986), 256 pp.
13. B.S. Kostin, E.V. Makienko, and I.E. Naats, in: *Problems of Remote Sensing of the Atmosphere* (IAO SB RAS, Tomsk, 1976), pp. 86–97.
14. I.E. Naats, *Theory of Multi–Frequency Laser Sounding of the Atmosphere* (Nauka, Novosibirsk, 1980), 157 pp.
15. A.N. Tikhonov and V.Ya. Arsenin, *Methods for Solving Ill-Posed Inverse Problems* (Nauka, Moscow, 1974) 203 pp.
16. V.V. Veretennikov, Atm. Opt. **3**, No. 10, 939–946 (1990).
17. O.D. Barteneva, N.I. Nikitinskaya, et al., *Transparency of the Atmospheric Column in Visible and IR Wavelength Range* (Gidrometeoizdat, Leningrad, 1991), 224 pp.
18. N.I. Nikitinskaya, O.D. Barteneva, and L.K. Veselova, Izv. Akad. Nauk SSSR, Fiz. Atmos. Okeana **9**, No. 4, 437–442 (1973)
19. H.J. Quenzel, Geophys. Res. **75**, No. 15, 21915–21921 (1970).